LANGMUIR Article
Cite This: Langmuir 2018, 34, 4142−4149
pubs.acs.org/Langmuir

Effect of Ethanolamines on the Electroless Deposition of Copper on Functionalized Organic Surfaces

Ashley A. Ellsworth[†,§] and Amy V. Walker*[,†,‡]

[†]Department of Chemistry and Biochemistry and [‡]Department of Materials Science and Engineering, University of Texas at Dallas, Richardson, Texas 75080, United States

Supporting Information

ABSTRACT: Electroless deposition (ELD) is widely used in industry to deposit metals because it is inexpensive and compatible with organic materials. The deposition rate and deposited film properties critically depend on the reducing agent, complexing agent, and bath pH and temperature as well as bath additives. We have investigated the role of ethanolamine additives in the ELD of copper using the reducing agent dimethylamine borane on $-CH_3$- and $-OH$-terminated self-assembled monolayers (SAMs) adsorbed on gold. Three additives were studied: ethanolamine (EOA), diethanolamine (DEOA), and triethanolamine (TEOA). Both the chemical identity and concentration of the ethanolamine significantly affect the deposition process. We show that the Cu deposition rate is faster on $-CH_3$-terminated surfaces than on $-OH$-terminated SAMs because of the stronger interaction of the ethanolamines with the hydroxyl terminal group. In contrast to physical vapor deposition and other ELD processes, Cu deposits atop methyl-terminated SAMs using TEOA. However, using EOA and DEOA, copper penetrates through $-CH_3$-terminated SAMs to the Au/S interface. For $-OH$-terminated SAMs, copper is observed to penetrate through the SAM for all ethanolamines investigated. The amount of copper penetration through the SAM to the Au/S interface increases with ethanolamine concentration. These effects are attributed to an adsorption−inhibition mechanism and differences in the chelation of Cu^{2+} in the deposition bath.

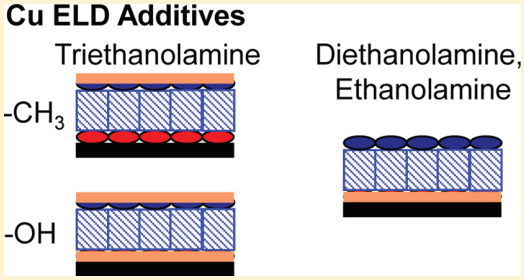

1. INTRODUCTION

Electroless deposition (ELD) of metals is widely employed in industrial processes for the metallization of organic substrates with applications in electronics,[1−4] electromagnetic interference shielding,[2,4] printed circuit boards,[4] fuel cells,[5] and sensors.[6] ELD occurs via the chemically promoted reduction of metals, that is, a REDOX reaction, without an externally applied potential. The deposition rate and deposited film properties therefore depend on the reducing agent, complexing agent, and bath pH and temperature.[2,7−13] For example, the rate of copper deposition using amine borane reducing agents is critically dependent on the strength of the B−N bond.[9,10] Complexing agents, such as ethylenediaminetetraacetic acid (EDTA), stabilize the bath and prevent the precipitation of metal hydroxides under alkaline conditions.[3,14] The choice of a complexing agent also affects the rate of deposition.[2,12,13] Finally, the interaction of the bath components with organic substrates can significantly affect the ELD process. A number of studies have demonstrated that stable, adherent metallic overlayers are produced if metal terminal group complexes are formed.[15−18] In recent studies, it has also been shown that the interaction of the reducing agent with the organic substrate affects deposition rates and deposited film properties.[10,17]

Additives are commonly employed in both electrodeposition and ELD to alter the physical and mechanical properties of deposits such as the grain size, brightness, electrical resistivity, hardness, and smoothness.[2,4,19,20] Examples include bis-(3-sulfopropyl)-disulfide,[21,22] 2-aminobenzothiazole,[23] benzotriazole,[21] polyethylene glycol,[1,4,14,23] dipyridyls,[3,24] saccharin,[25] adenine,[11,18,25] guanine,[11,18,25] and 3-mercapto-1-propanesulfonate.[22,26] Additionally, additives can accelerate or inhibit the rate of deposition.[1,4,11,21,27] There have been very few systematic studies of the effect of additive structure on the film deposition rate or properties. Kondo and co-workers[12,13] have demonstrated that for the tertiary amines, nitriloacetic acid (NTA), triethanolamine (TEOA), and triisopropanolamine, there were large differences in the rate of copper ELD using the reducing agent formaldehyde. These authors observed that using TEOA, the rate of deposition was ∼20× faster than using EDTA alone. Further, the rate of deposition passed through a maximum as the additive concentration increased. These studies suggest that both the interaction of the ligand with the surface and the chemical structure of the Cu(II) complex are important in ELD processes. However, although these additives are all tertiary amines, they exhibit very different pK_a's,[28−30] and in the case of NTA multiple pK_a's,[28] which complicates analysis of the data.

Received: October 26, 2017
Revised: February 13, 2018
Published: March 12, 2018

DOI: 10.1021/acs.langmuir.7b03725
Langmuir 2018, 34, 4142−4149

Ethanolamines combine the properties of amines and alcohols and therefore have a variety of industrial applications as lubricants, surfactants, and herbicides and in gas purification.[31,32] They are versatile ligands that behave as N and O donors[20] and easily form complexes with transition metals.[20,33−39] In ELD and electroplating, ethanolamines have been reported to act as both complexing agents and buffers.[2,3,7,12,13,27] A number of studies have reported that TEOA increases the rate of copper deposition which has been attributed to the formation of Cu(II)−TEOA complexes or mixed ligand species (in the presence of other complexing agents).[2,7,12,13,27] TEOA can also slow the metal deposition rate by adsorbing onto the sample, which inhibits the oxidation of reducing agents, such as formaldehyde.[13,27] The properties of the deposited film are also altered by TEOA; the grain size is observed to decrease while the electrical resistivity is improved.[2] There have been far fewer studies of the effect of ethanolamine (EOA) or diethanolamine (DEOA) on ELD and electroplating.[20,40] Hammami and co-workers[20] observed differences in the morphologies of electroplated Zn−Ni films using DEOA and TEOA. Using DEOA, the films had a nodular morphology with agglomeration of grains, while the Zn−Ni deposit was composed of triangular-based pyramidal grains when TEOA was employed. Further, the corrosion resistance of the films improved using TEOA but was not improved using DEOA.

In this paper, we systematically investigate the role of the ethanolamine structure on copper ELD using the reducing agent dimethylamine borane (DMAB) on functionalized organic thin films. EOA, DEOA, and TEOA are primary, secondary, and tertiary amines, respectively, but have similar pK_a's.[29,41,42] We employ hydroxyl- and methyl-terminated alkanethiolate self-assembled monolayers (SAMs) adsorbed on gold as model organic substrates. This is because SAMs are well-ordered with a uniform density of terminal groups.[43−45] Hydroxyl and methyl terminal groups were chosen because their surfaces are hydrophilic and hydrophobic, respectively, and do not change their protonation under experimental conditions commonly employed in ELD. Our data indicate that the choice of ethanolamine is critical; both the chemical identity and concentration of the EOA significantly affect the deposition process. We demonstrate that the Cu deposition rate is faster on $-CH_3$-terminated SAMs than on −OH-terminated SAMs because of the stronger interaction of the ethanolamines with the hydroxyl terminal group. We further show that Cu only deposits atop methyl-terminated SAMs using TEOA. Using EOA and DEOA, copper penetrates through $-CH_3$-terminated SAMs to the Au/S interface. For −OH-terminated SAMs, copper is observed to penetrate through the SAM for all the ethanolamines studied. Further, the amount of copper penetration increases with ethanolamine concentration. We propose that these effects can be described using an adsorption−inhibition mechanism and differences in the formation of mixed complexes of Cu^{2+} with EOA, DEOA, TEOA, and EDTA.

2. EXPERIMENTAL SECTION

2.1. Materials. Gold (99.995%), chromium (99.995%), EOA (99+%), and TEOA (98+%) were acquired from Alfa Aesar, Inc. (Ward Hill, MA). Copper(II) sulfate pentahydrate ($CuSO_4{\cdot}5H_2O$, 98+%), EDTA (98%), DMAB complex (97%), and hexadecanethiol (HDT) (99+%) were purchased from Sigma-Aldrich, Inc. (St. Louis, MO). 16-Hydroxy-1-HDT (MHL) (99+%) was obtained from Frontier Scientific (Logan, UT). DEOA (>99%) was acquired from TCI America (Portland, OR). Anhydrous ethanol (ACS grade) was purchased from Aaper Alcohol (Shelbyville, KY). Concentrated sulfuric acid (95%) was purchased from BDH Aristar, Inc. (Chester, PA). All reactants were used without further purification. Silicon wafers (⟨111⟩ orientation) were acquired from Addison Engineering Inc. (San Jose, CA) and cleaned using RCA SC-1 etch (H_2O/NH_4OH/H_2O_2 = 5:1:1) for 20 min prior to use.

2.2. Preparation of SAMs. The preparation of SAMs has been described in detail previously.[46,47] In brief, chromium (∼50 Å) and then gold (∼1000 Å) were sequentially thermally deposited onto clean Si wafers. Well-ordered SAMs were then formed by immersing the gold substrate into 1 mM ethanolic solutions of the appropriate alkanethiol for 24 h at ambient temperature (22 ± 1 °C). The samples were then rinsed with ethanol and dried under N_2 gas. To further investigate the adhesion of the deposited copper layer, ethanolic solutions of 0.5 mM MHL and 0.5 mM HDT (total alkanethiol concentration = 1 mM) were also used to prepare SAMs using the same procedure. For each batch, one sample was taken and characterized using single-wavelength ellipsometry (Gaertner Scientific Corp., Skokie, IL) and time-of-flight secondary ion mass spectrometry (TOF SIMS) to ensure that the SAMs were free of significant chemical contamination.

2.3. Copper ELD. The standard "100%" copper ELD solution was composed of 0.032 M copper(II) sulfate pentahydrate, 0.3 M ethanolamine (either EOA, DEOA, or TEOA), 0.037 M EDTA, and 0.067 M DMAB. To study the effect of the ethanolamine concentration on Cu ELD, the ethanolamine concentration was altered while keeping the other reagent concentrations constant. The ethanolamine concentrations are reported as a percentage of the standard concentration (0.3 M). The pH reported was adjusted to pH 9 using dilute sulfuric acid before addition of the reducing agent, DMAB. All experiments were carried out at room temperature (22 ± 1 °C). Depositions were performed for periods of time ranging from 7 min to 1.5 h. After deposition, each substrate was rinsed with deionized water and ethanol and dried with N_2 gas. The resulting films were immediately studied using TOF SIMS and optical microscopy.

2.4. Time-of-Flight Secondary Ion Mass Spectrometry. TOF SIMS measurements were performed using an ION TOF IV spectrometer (ION TOF Inc., Chestnut Hill, NY) with a Bi liquid metal ion gun primary ion source. The instrument has three chambers for sample introduction, preparation, and analysis. The pressure of the analysis and preparation chambers is typically less than 5×10^{-9} mbar. The Bi^+ primary ions had a kinetic energy of 25 keV. The probe beam diameter was ∼100 nm and rastered over a (500 × 500) μm^2 area during data acquisition. The spectra were acquired using an ion dose of less than 10^{11} ions cm^{-2}, which is within the static regime.

For each experiment, a minimum of three samples were made and three separate areas on each sample were analyzed. The reported data therefore represent an average of at least nine measurements, and the error bars represent the corresponding standard deviation.

2.5. Optical Microscopy. Optical microscopy was performed using a Keyence VHX-2000 digital microscope. Dark-field images were acquired with 200× magnification. The images shown are representative of the data obtained.

3. RESULTS AND DISCUSSION

3.1. Bare SAMs. The positive and negative secondary ion mass spectra of −OH- and $-CH_3$-terminated SAMs have been reported in detail previously.[46,47] Briefly, in the negative ion spectra, a number of high mass cluster ions are observed such as $Au_xS_y^-$, AuM_2^-, and Au_2M^-, where M is the intact alkanethiolate adsorbate species. Fragment ions are also observed that are indicative of the SAM terminal group and methylene backbone, for example, $(CH_2)_xS_y^-$. In the positive ion mass spectra, a number of characteristic ions are also observed including $(CH_2)_x(CH)_y^+$, $S(CH_2)_x^+$, and $[AuS(CH_2)_x]H^+$.

DOI: 10.1021/acs.langmuir.7b03725
Langmuir 2018, 34, 4142−4149

Table 1. Fragment and Cluster Ions Observed in the TOF SIMS Spectra of Both $-CH_3$- and $-OH$-Terminated SAMs, Only $-CH_3$-Terminated SAMs, and Only $-OH$-Terminated SAMs after Cu ELD Using TEOA, DEOA, and EOA

	fragment ions observed		
ethanolamine	on both $-CH_3$- and $-OH$-terminated SAMs	only on $-CH_3$-terminated SAM	only on $-OH$-terminated SAM[a]
EOA	Cu_x^+ (x = 1–3), $CuSH_2^+$, $Au_xCu_yS_z^\pm$	$AuCuS(CH_2)_x^+$, $Au_xCuS(CH_2)_x^-$	$Au_xCuS(CH_2)_x^\pm$, $[AuCu(MHL-H)]^-$
DEOA	Cu_x^+ (x = 1–3), $CuSH_2^+$, $Au_xCu_yS_z^\pm$	$Au_xCuS(CH_2)_x^-$, $Cu_3SH_2^+$	$Au_xCuS(CH_2)_x^\pm$, $[AuCu(MHL-H)]^-$, $CuO(CH_2)_x^+$, CuO^-, $CuOH^\pm$
TEOA	Cu_x^+ (x = 1–3)	$Cu(CH_2)_x(CH_3)^+$ (x = 1–4)	$CuSH_2^+$, $Au_xCu_yS_z^\pm$, $Au_xCuS(CH_2)_x^-$, $CuS(CH_2)_xCH^+$, $CuO(CH_2)_x^+$, CuO^-, $CuOH^\pm$, $Cu_4OH(CH_2)^-$

[a]MHL = $-S(CH_2)_{15}OH$.

3.2. Copper Deposition. For all ethanolamines studied, copper was observed to deposit on both $-OH$- and $-CH_3$-terminated SAMs. Table 1 summarizes the fragment and cluster ions observed in the TOF SIMS spectra upon Cu ELD using different ethanolamines.

The data indicate that for methyl-terminated SAMs, Cu is deposited atop the SAM if TEOA is employed as a bath additive. We observe ions of the form $[Cu_4(CH_2)_xCH_3]^+$, indicating that Cu interacts with the methyl terminal group, but no $Au_xCu_yS_z^\pm$ ions could be observed, which are characteristic of metal atom penetration through the SAM to the Au/S interface. Using EOA and DEOA, ions of the forms $Au_xCu_yS_z^\pm$ and $Au_xCu_yS_z(CH_2)_a^-$ are observed, indicating that some copper has penetrated through the methyl-terminated SAM to the Au/S interface. Similar to previous studies using physical vapor deposition[48] and ELD,[10] the data indicate that copper both deposits atop $-OH$-terminated SAMs and penetrates to the Au/S interface for all ethanolamines investigated. In the SIMS spectra, ions of the forms $CuO(CH_2)_x^+$ and $Cu_x(OH)^\pm$ are observed, indicating that deposited Cu has interacted with the $-OH$ terminal group, whereas ions of the form $Au_xCu_yS_z^\pm$ indicate that copper has also penetrated to the Au/S interface.

It is interesting to note that only ions containing four copper atoms are observed after Cu ELD on $-CH_3$- and $-OH$-terminated SAMs using TEOA (Table 1, Figure 1 and Supporting Information S1). Figure 1 displays the ion intensities of $Cu_4(CH_3)_2^+$ upon Cu ELD on $-CH_3$-terminated SAMs using different ethanolamines. It can be seen that only Cu_4-containing clusters are observed if TEOA is employed as a bath additive. This is also the only system in which copper deposits atop the SAM only. This suggests that the critical nucleus for copper ELD atop functionalized SAMs is Cu_4. If copper formed in the ELD reaction adsorbs on a copper island which is smaller than the critical nucleus size, it is not stable on the SAM surface and will penetrate through the SAM to the Au/S interface. To test this hypothesis, we examined the intensities of $Cu_4(CH_2)_y(CH_3)_y^+$ with deposition time. By the classical nucleation theory, if a Cu tetramer cluster is the critical nucleus, it is expected that the ion intensities of the Cu_4-containing ions would increase with deposition time and then decrease as the film forms. Our data clearly indicate that the ion intensity of $Cu_4(CH_3)_2^+$ increases with deposition time and then decreases as the Cu film forms (Supporting Information Figure S2). Similarly, on $-OH$-terminated SAMs, the ion intensity of $[Cu_4OH(CH_2)]^-$ increases with deposition time (data not shown). Thus, it is likely that the critical nucleus size for Cu deposition atop the SAM is a Cu tetramer.

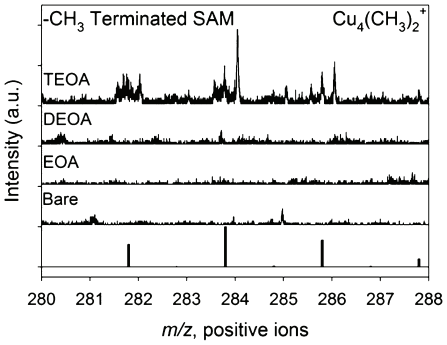

Figure 1. High-resolution positive ion spectra centered at m/z 284 after Cu ELD on a $-CH_3$-terminated SAM using EOA, DEOA, and TEOA. Deposition conditions: pH 9, 22 °C. For reference, the mass spectrum of the bare SAM ("Bare") and the calculated isotopic distribution of $Cu_4(CH_3)_2^+$ are also shown.

Dark-field optical microscopy can also be employed to provide information about the deposited films. Ellsworth and Walker[10] observed that for Cu ELD on $-CH_3$, $-OH$, and $-COOH$, the deposited Cu film appeared to be quite uniform if copper deposited atop the functionalized SAM. In contrast, the Cu film appeared to be nonuniform if some of the Cu penetrated to the Au/S interface. Figure 2 displays the dark-field optical images after Cu ELD on $-CH_3$- and $-OH$-terminated SAMs using TEOA, DEOA, and EOA as bath additives. The data are consistent with the SIMS spectra. On $-CH_3$-terminated SAMs using TEOA, the deposited film appears to be quite uniform and indicate that the copper film has deposited atop the SAM. Using EOA and DEOA, the Cu deposit appears to be nonuniform; large copper islands are observed. On $-OH$-terminated SAMs for all ethanolamines studied, the deposited Cu films are also nonuniform with large islands. These observations indicate that some of the deposited Cu has penetrated through the SAM to the Au/S interface.

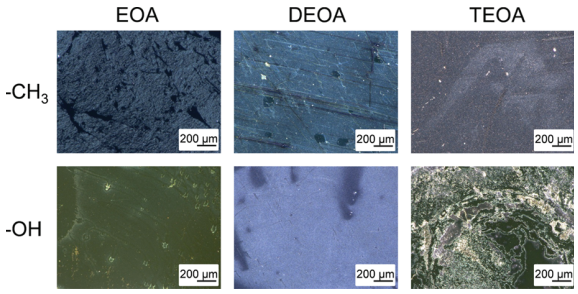

Figure 2. Dark-field optical images of the deposited copper layer after Cu ELD using EOA, DEOA, and TEOA on $-CH_3$- and $-OH$-terminated alkanethiolate SAMs. Deposition conditions: pH 9, 22 °C.

DOI: 10.1021/acs.langmuir.7b03725
Langmuir 2018, 34, 4142–4149

Table 2. Variation of the Time (min) for a Copper Layer To Deposit That Is Visible to the Naked Eye with Ethanolamine Concentration on $-CH_3$- and $-OH$-Terminated SAMs[a]

	deposition time (min)									
	concentration (%)	50	100	150	50	100	150	50	100	150
SAM terminal group	ethanolamine		EOA			DEOA			TEOA	
$-CH_3$		10	18	36	18	18	29	10	20	7
$-OH$		18	90	42	27	32	42	12	25	11

[a]The concentrations are reported as a percentage of the "standard" ethanolamine concentration, 0.3 M.

3.3. Variation of Copper Deposition with EOA Identity and Concentration. The data clearly indicate that copper ELD on $-CH_3$- and $-OH$-terminated SAMs is dependent on both the SAM terminal group and the chemical identity of the ethanolamine. To further investigate the effect of the ethanolamine on Cu ELD, the ethanolamine concentration was varied from 0.15 M ("50%") to 0.45 M ("150%"). Table 2 shows the deposition time (to the nearest minute) required to deposit a copper layer that is visible to the naked eye.

In general, the deposition time is longer on $-OH$-terminated SAMs than on $-CH_3$-terminated SAMs. Further, the deposition time using EOA and DEOA generally increases with ethanolamine concentration. However, the deposition time appears to initially increase and then decrease with TEOA concentration. Interestingly, for all ethanolamines investigated, the copper deposit does not adhere to the SAMs at 50% concentration (0.15 M); the copper deposit can easily be removed via rinsing with solvents such as ethanol and water and using the tape test. It is currently unclear why this occurs, and we are currently performing further studies to understand this effect.

Further information about the deposition can be obtained by examining the intensities of the molecular cluster ions, such as Au_2M^-, which involve the absorbed intact SAM molecule (M). For $-CH_3$-terminated SAMs, the ion intensity of Au_2M^- (M = $-S(CH_2)_{15}CH_3$; Figure 3a) increases with increasing ethanolamine concentration, indicating that more methyl-terminated SAM molecules are chemically intact after Cu deposition. This observation suggests that as the ethanolamine concentration increases, it interacts with more $-CH_3$-terminated SAM preventing copper deposition and leads to the formation of copper islands. For $-OH$-terminated SAMs, the ion intensity of Au_2M^- (M = $-S(CH_2)_{15}CH_2OH$) remains approximately constant with increasing ethanolamine concentration (Figure 3b), which suggests that the interaction of the ethanolamines is independent of concentration and may be quite strong.

To test whether $-OH$-terminated SAMs interact strongly with the ethanolamine additives but the $-CH_3$-terminated SAMs do not (and so their interaction is dependent on the ethanolamine concentration), the deposition was carried out without the copper source ($CuSO_4$). After the reaction on $-CH_3$-terminated SAMs, few differences are observed between the "as-deposited" and bare $-CH_3$-terminated SAM mass spectra, confirming that there is little interaction between the $-CH_3$-terminated SAM and the ethanolamines (Figure 4a). For $-OH$-terminated SAMs, many ions indicative of the interaction of the ethanolamine with the SAM are observed (Figure 4b), confirming that the polar ethanolamines interact more strongly with the hydroxyl-terminated SAM surface.

The ion intensities of $Au_xCu_yS_z^{\pm}$ and Cu_x^+ (x = 1–3) are indicative of the amount of copper penetration through the layer. Figure 5 displays the variation of $AuCuS^-$ ion intensity

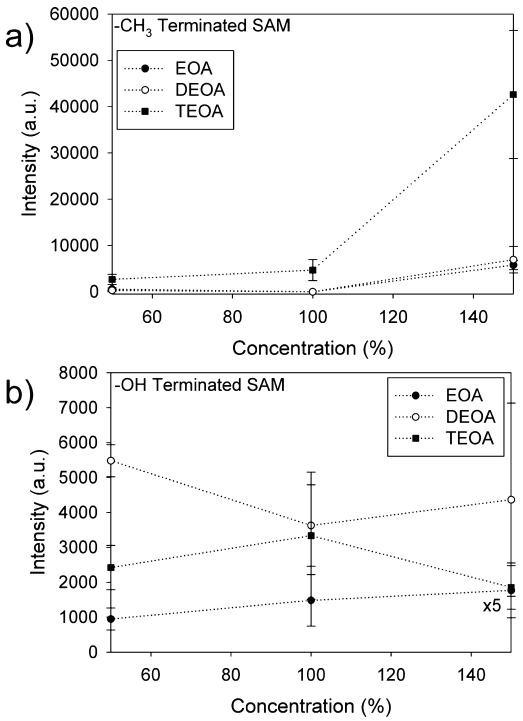

Figure 3. Integrated ion intensities (peak areas) of Au_2M^- after Cu ELD using EOA, DEOA, and TEOA: (a) $-CH_3$ (M = $-S(CH_2)_{15}CH_3$, m/z 651) and (b) $-OH$ (M = $-S(CH_2)_{15}CH_2OH$, m/z 667) alkanethiolate SAMs. The dotted lines are shown as guides to the eye.

(peak area) with ethanolamine concentration after Cu ELD on $-CH_3$- and $-OH$-terminated SAMs. On $-CH_3$-terminated SAMs for TEOA, the $AuCuS^-$ ion intensity is zero, indicating that copper does not penetrate through the SAM for all ethanolamine concentrations tested. However, for EOA and DEOA, it can be clearly seen that the ion intensity of $AuCuS^-$ increases with ethanolamine concentration. On $-OH$-terminated SAMs, the $AuCuS^-$ ion intensity is the smallest at 150% ethanolamine concentration, indicating that the ethanolamines block metal atom penetration through the $-OH$-terminated SAM to the Au/S interface. We note that a similar behavior has been observed for Cu ELD on $-COOH$-terminated SAMs using formaldehyde as a reducing agent and the additive adenine.[18]

The ion intensities of the copper cluster ions, Cu_x^+ (x = 1–3), are consistent with the above observations (Supporting Information Figure S3). Previous studies by Allara, Winograd, Walker and co-workers[46−49] that show metal cluster ion intensities differ between systems where metals deposit on functionalized SAM surfaces and systems where metals penetrate through the monolayer. It was observed that for

DOI: 10.1021/acs.langmuir.7b03725
Langmuir 2018, 34, 4142−4149

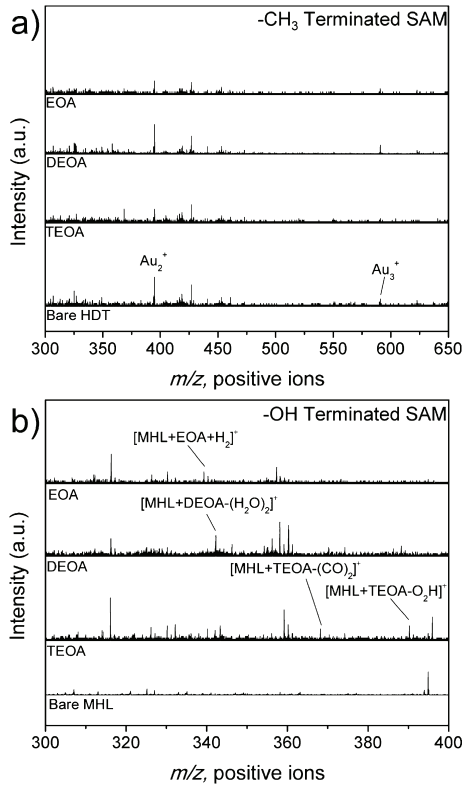

Figure 4. High-resolution positive ion mass spectra after Cu ELD without the addition of the Cu source, $CuSO_4$, using EOA, DEOA, and TEOA: (a) $-CH_3$ (M = $-S(CH_2)_{15}CH_3$) and (b) $-OH$ (M = $-S(CH_2)_{15}CH_2OH$) alkanethiolate SAMs.

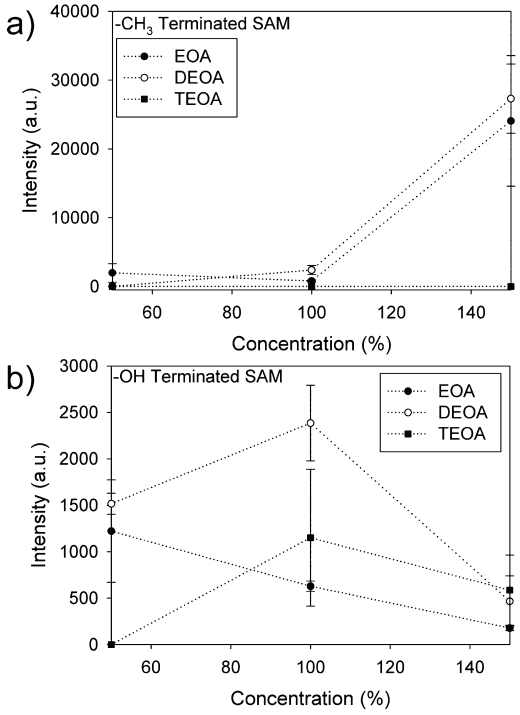

Figure 5. Integrated ion intensities (peak areas) of $AuCuS^-$ after Cu ELD using EOA, DEOA, and TEOA: (a) $-CH_3$ (M = $-S(CH_2)_{15}CH_3$) and (b) $-OH$ (M = $-S(CH_2)_{15}CH_2OH$). The dotted lines are shown as guides to the eye.

vapor-deposited metals, including Al, Ag, and Cu, which chemisorb at the SAM/vacuum interface, the ion intensities of M_x^+ (x = 2, 3; M = metal of interest) were relatively low. The ion intensities of these cluster ions were much larger if some of the metals penetrated through the functionalized SAM to the Au/S interface. Using TEOA, the relative ion intensities of Cu_2^+ and Cu_3^+ are very small. For $-CH_3$-terminated ions, these ions are ~0.5% of the Cu^+ ion intensity, while on $-OH$-terminated SAMs, the relative ion intensities of Cu_2^+ and Cu_3^+ to Cu^+ are between ~1 and ~5%. Using DEOA and EOA, the relative ion intensities of Cu_2^+ and Cu_3^+ are much larger. In general, the relative ion intensities for these cluster ions are the largest for EOA. For $-OH$-terminated SAMs, the relative ion intensities of Cu_2^+ and Cu_3^+ are between ~10 and ~235% of the Cu^+ ion intensity. On $-CH_3$-terminated SAMs, the relative ion intensities of Cu_2^+ and Cu_3^+ are generally smaller between ~20 and ~120% of the Cu^+ ion intensity. Taken together, the data indicate that using TEOA, copper deposits atop $-CH_3$-terminated SAMs while some copper penetrates through the $-OH$-terminated SAM to the Au/S substrate. For DEOA and EOA, the ion intensities of Cu_x^+ indicate that the deposited copper penetrates through both $-CH_3$- and $-OH$-terminated SAMs.

3.4. Reaction Pathways in the ELD of Copper on Functionalized SAMs. Any proposed reaction mechanism for the effect of ethanolamines on Cu ELD on functionalized SAMs must account for the following experimental observations:

(a) The deposition rate is faster on $-CH_3$-terminated SAMs than $-$on OH-terminated SAMs;
(b) For EOA and DEOA, the deposition rate increases with increasing ethanolamine concentration;
(c) The deposition rate appears to decrease and then increase again with TEOA concentration;
(d) Copper penetrates through $-OH$-terminated SAMs to the Au/S interface for all ethanolamines studied; and
(e) Copper deposits atop $-CH_3$-terminated SAMs using TEOA but penetrates through the SAM to the Au/S interface using EOA or DEOA.

These observations may seem surprising because $-CH_3$-terminated SAMs are hydrophobic, and therefore, one would expect the deposition rate on $-OH$-terminated SAMs to be faster. Second, previous studies have shown that metals generally penetrate through methyl-terminated SAMs.[18,46−49] Third, the ethanolamines act as additives and do not participate in the ELD reaction directly. ethanolamines also have a significantly lower association constant with Cu^{2+} ions than EDTA, which is also present in the solution.[39,50] Further, the deposition behavior is observed to be different using TEOA than using EOA and DEOA. Thus, any proposed reaction pathway must take into account both the chemical identity of the ethanolamine additive and the surface.

The ELD of copper using DMAB can be described by the following reaction equation[51]

$$3Cu^{2+}(aq) + (CH_3)_2NHBH_3(aq) + 3H_2O(l) \rightarrow 3Cu(s) + (CH_3)_2NH_2^+(aq) + H_3BO_3(aq) + 5H^+(aq) \quad (1)$$

The ELD of metals using amine borane reducing agents has been extensively studied.[3,9−11,17,52−54] Walker and co-workers have attributed the difference in the ELD rates of metals on

DOI: 10.1021/acs.langmuir.7b03725
Langmuir 2018, 34, 4142−4149

$-CH_3$- and $-OH$-terminated SAMs to the interaction of the SAM terminal with the reducing agent, DMAB.[10,17,52,53] Briefly, the difference in the ELD rates on $-OH$- and $-CH_3$-terminated SAMs can be accounted in the following way. The initial step in deposition using amine boranes is believed to be the adsorption of the reducing agent, followed by cleavage of the N−B bond.[9,51,54] For DMAB, the (unbalanced) reaction equation for this process is

$$\begin{aligned}&(CH_3)_2NHBH_3(aq)\\ &\rightarrow (CH_3)_2NHBH_3(ads) + H^+(aq)\\ &\rightarrow (CH_3)_2NH_2{}^+(aq) + BH_3(ads)\end{aligned} \quad (2)$$

where ads indicates a species adsorbed on the substrate. In the above reaction (eq 2), the dimethylamine fragment ($(CH_3)_2NH$) acts as a Lewis base and hence reacts with protons present in the deposition bath to form soluble $(CH_3)_2NH_2{}^+$ species. The BH_3 group acts as a Lewis acid and therefore has a slight negative charge.[10] The C−OH terminal bond of the hydroxyl-terminated SAM is covalent and polar with the $-OH$ group having a partial negative charge (δ^-). For methyl-terminated SAMs, the C−H terminal group bonds are not polar and have no partial charge. Thus, BH_3 is repelled by the $-OH$-terminated surface while the BH_3 fragment is able to easily adsorb on the $-CH_3$-terminated surface. Because the BH_3 fragment acts as the reducing agent in the ELD reaction (eq 1), deposition begins at slightly later times on hydroxyl-terminated SAMs than on methyl-terminated SAMs.[10] Thus, the deposition times observed on $-OH$-terminated SAMs are longer than on $-CH_3$-terminated SAMs (Table 2).

However, the interaction of the BH_3 fragment alone with the SAM terminal groups alone cannot explain our observations; the deposition is also dependent on both the chemical identity and concentration of the ethanolamines. For EOA and DEOA, the deposition rates decrease (Table 2; deposition time increases) with increasing ethanolamine concentration and can be explained by an adsorption−inhibition mechanism.[13] In this reaction pathway, excess ethanolamine present in solution adsorbs on the SAM surface, which inhibits the (heterogeneous) Cu ELD reaction (most likely by sterically hindering the deposition reaction[13]). Assuming that the surface coverage of the ethanolamines is proportional to their concentration in solution, as the concentration of EOA and DEOA increases there is a higher coverage of the ethanolamines on the SAM surface, which blocks the deposition of copper. Hence, as the concentration of EOA and DEOA increases, the copper deposition rate decreases. This mechanism also explains the slower deposition of copper on $-OH$-terminated SAMs than on $-CH_3$-terminated SAMs (Table 2). The ethanolamines interact more strongly with the hydroxyl terminal group than the methyl terminal group (Figure 4). Hence, at a given ethanolamine concentration, there is a higher ethanolamine coverage present on the $-OH$-terminated SAM, leading to a stronger inhibition effect and a slower Cu ELD rate.

Using TEOA, we observe different behaviors; for both $-CH_3$- and $-OH$-terminated SAMs, the deposition rate is generally faster using TEOA than using DEOA and EOA and appears to decrease and then increase again as the TEOA concentration increases (Table 2). There are a number of possible reasons for this behavior including differences in the complexing ability of ethanolamines toward copper(II) ions and the interaction of copper(II)−TEOA complexes with the SAM surface. There have been a number of studies of the formation of copper complexes with ethanolamines[33−38] using methods including polarography, spectrophotometry, potentiometry, and electron spin resonance spectroscopy. These studies show that there are differences in the structure and formation constants of copper complexes with EOA, DEOA, and TEOA.[34−39] Below pH ≈ 12, EOA and DEOA are believed to form complexes with Cu^{2+} via the stepwise addition of two ligands to the metal center, followed by deprotonation of the two hydroxyl groups and chelation. For TEOA, only one ligand is added to the Cu^{2+} ion because of steric hindrance effects. Subsequently, there is deprotonation of one of the hydroxyl groups and chelation of the metal ion. These $CuLH_{-1}$ (where L = TEOA) complexes easily form dimers, and there is a subsequent deprotonation of other hydroxyl groups to form $Cu_2L_2H_{-4}$. The formation constant for the Cu(II)−TEOA dimer, $10^{-1.42}$,[39] is much larger than the formation constants of copper(II) complexes with EOA and DEOA, $10^{-8.06}$ and $10^{-6.97}$ respectively,[39] suggesting that there are more copper(II)−TEOA complexes present in the deposition bath at a given ethanolamine concentration. However, the presence of EDTA and the solution pH (pH 9) affects the formation of such complexes. The complexing constant of EDTA with copper is much larger than that of the ethanolamines,[50] indicating that the concentration of copper(II)−EDTA complexes is significantly higher. Under our experimental conditions, it has been reported that both EDTA and ethanolamines form mixed ligand complexes with high formation constants.[33,34,38,55,56] Indeed, in recent studies, Wang et al.[27] also observed that in copper ELD, the deposition rate of copper increased and then decreased with TEOA concentration. This effect was attributed to the presence of a mixed EDTA and TEOA complex, $[Cu(EDTA)(TEA)_2]^{2-}$, which shifted the reduction potential of $[Cu(EDTA)]^{2-}$ to a more positive value, making it easier to reduce Cu^{2+} to copper metal. Further, we also expect that the concentration of ions, that is, complexes, is different from that in the bulk solution because of the electrical double layer that forms close to the substrate.

For TEOA, we therefore propose that the deposition reaction occurs in the following way. First, we assume that the reduction of the adsorbed copper(II) complexes by DMAB is only effective when the surface is bare and able to adsorb DMAB from any direction. This assumption seems reasonable because it is believed that the first step in the ELD of metals using amine boranes is the dissociative adsorption of reductant to form the corresponding amine and borane (BH_3) fragments (eq 2).[9,51,54] If the surface is covered by TEOA, the dissociative adsorption of the amine borane is sterically hindered, leading to a reduced reaction rate. Thus, as the TEOA concentration increases, there is an initial decrease in the reaction rate because excess TEOA adsorbs on the SAM surface which inhibits Cu ELD. At higher TEOA concentrations, there is a significant increase in the concentration of a mixed ligand complex, $[Cu(EDTA)(TEA)_2]^{2-}$;[27] these are able to easily adsorb on the SAM surface, leading to more copper being available for the reaction. Thus, the apparent reaction rate increases slightly at higher TEOA concentrations.[27] As the concentration of TEOA increases further, the deposition of copper decreases because the TEOA surface coverage is sufficient to inhibit deposition. The proposed reaction pathway is also consistent with the slower deposition of copper on $-OH$-terminated SAMs than on $-CH_3$-terminated SAMs. There is a stronger interaction of

DOI: 10.1021/acs.langmuir.7b03725
Langmuir 2018, 34, 4142−4149

the hydroxyl terminal group with TEOA (Figure 4) than the methyl terminal group with TEOA, and thus, there is a higher surface coverage of TEOA on the −OH-terminated SAM. This leads to a slower Cu ELD rate on −OH-terminated SAMs because the reaction is more sterically hindered on this surface.

4. CONCLUSIONS

Copper ELD is strongly dependent on the ethanolamine additive employed; the chemical identity and concentration of the ethanolamine significantly affect the deposition process. The Cu deposition rate is faster on $-CH_3$-terminated SAMs than on −OH-terminated SAMs because of the stronger interaction of the ethanolamines with the hydroxyl terminal group.

The deposition mechanism is different using TEOA than using DEOA and EOA. This is likely due to the different chelation properties of TEOA. Using TEOA, Cu only deposits atop $-CH_3$-terminated SAMs, whereas using both EOA and DEOA, copper both deposits on top of the SAM and penetrates through the SAMs to the Au/S interface. For −OH-terminated SAMs, copper is observed to penetrate through the SAM for all ethanolamines studied. Further, the amount of copper penetration increases with ethanolamine concentration. We propose that these effects can be described using an adsorption−inhibition mechanism in which as the ethanolamine concentration increases, it blocks the Cu ELD reaction and subsequent deposition of copper on the SAM. For TEOA, the formation of mixed ligand complexes aids in the copper deposition reaction because they can easily adsorb to the SAM surface, leading to more copper being available for the reaction.

■ ASSOCIATED CONTENT

Supporting Information

The Supporting Information is available free of charge on the ACS Publications website at DOI: 10.1021/acs.langmuir.7b03725.

High mass resolution negative ion spectra centered at m/z 327 after Cu ELD on −OH-terminated SAMs using EOA, DEOA, and TEOA; variation of $Cu_4(CH_3)_2^+$ with deposition time on a $-CH_3$-terminated SAM using TEOA; and variation of the Cu_x^+ (x = 1−3) ion intensities with ethanolamine concentration on $-CH_3$- and −OH-terminated SAMs (PDF)

■ AUTHOR INFORMATION

Corresponding Author

*E-mail: amy.walker@utdallas.edu. Phone: +1 972 883 5780. Fax: +1 972 883 5725.

ORCID

Ashley A. Ellsworth: 0000-0001-8912-3645

Amy V. Walker: 0000-0003-2114-3644

Present Address

§Physical Electronics, Inc., 18725 Lake Drive East, Chanhassen, MN 55317, USA.

Author Contributions

The manuscript was written through contributions of all authors.

Funding

National Science Foundation CHE 1213546, CHE 1708259.

Notes

The authors declare no competing financial interest.

■ ACKNOWLEDGMENTS

The authors gratefully acknowledge the support from the National Science Foundation (CHE 1213546 and CHE 1708258).

■ REFERENCES

(1) Hasegawa, M.; Yamachika, N.; Okinaka, Y.; Shacham-Diamand, Y.; Osaka, T. An Electrochemical Investigation of Additive Effect in Trench-Filling of ULSI Interconnects by Electroless Copper Deposition. *Electrochemistry* **2007**, *75*, 349−358.

(2) Lin, Y.-M.; Yen, S.-C. Effects of additives and chelating agents on electroless copper plating. *Appl. Surf. Sci.* **2001**, *178*, 116−126.

(3) Jagannathan, R.; Krishnan, M. Electroless plating of copper at a low pH level. *IBM J. Res. Dev.* **1993**, *37*, 117−123.

(4) Gan, X.; Zhou, K.; Hu, W.; Zhang, D. Role of additives in electroless copper plating using hypophosphite as reducing agent. *Surf. Coat. Technol.* **2012**, *206*, 3405−3409.

(5) Poon, K. C.; Tan, D. C. L.; Vo, T. D. T.; Khezri, B.; Su, H.; Webster, R. D.; Sato, H. Newly Developed Stepwise Electroless Deposition Enables a Remarkably Facile Synthesis of Highly Active and Stable Amorphous Pd Nanoparticle Electrocatalysts for Oxygen Reduction Reaction. *J. Am. Chem. Soc.* **2014**, *136*, 5217−5220.

(6) Hilmi, A.; Luong, J. H. T. Electrochemical Detectors Prepared by Electroless Deposition for Microfabricated Electrophoresis Chips. *Anal. Chem.* **2000**, *72*, 4677−4682.

(7) Li, J.; Kohl, P. A. Complex Chemistry & the Electroless Copper Plating Process. *Plat. Surf. Finish.* **2004**, *91*, 40−43.

(8) Duffy, J.; Pearson, L.; Paunovic, M. The Effect of pH on Electroless Copper Deposition. *J. Electrochem. Soc.* **1983**, *130*, 876−880.

(9) Lelental, M. Effect of amine borane structure on activity in electroless plating. *J. Catal.* **1974**, *32*, 429−433.

(10) Ellsworth, A. A.; Walker, A. V. Role of the Reducing Agent in the Electroless Deposition of Copper on Functionalized SAMs. *Langmuir* **2017**, *33*, 8663−8670.

(11) Paunovic, M. Electroless Deposition of Copper. In *Modern Electroplating*, 4th ed.; Schlesinger, M.; Paunovic, M., Eds.; John Wiley & Sons: New York, 2000; pp 645−665.

(12) Kondo, K.; Ishikawa, J.; Takenaka, O.; Matsubara, T.; Irie, M. Electroless Copper Plating in the Presence of Excess Triethanol Amine. *J. Electrochem. Soc.* **1990**, *137*, 1859−1860.

(13) Kondo, K.; Ishikawa, J.; Takenaka, O.; Matsubara, T.; Irie, M. Acceleration of Electroless Copper Deposition in the Presence of Excess Triethanolamine. *J. Electrochem. Soc.* **1991**, *138*, 3629−3633.

(14) Li, J.; Kohl, P. A. The Acceleration of Nonformaldehyde Electroless Copper Plating. *J. Electrochem. Soc.* **2002**, *149*, C631−C636.

(15) Garno, J. C.; Zangmeister, C. D.; Batteas, J. D. Directed Electroless Growth of Metal Nanostructures on Patterned Self-Assembled Monolayers. *Langmuir* **2007**, *23*, 7874−7879.

(16) Zangmeister, C. D.; van Zee, R. D. Electroless Deposition of Copper onto 4-Mercaptobenzoic Acid Self-Assembled on Gold. *Langmuir* **2003**, *19*, 8065−8068.

(17) Shi, Z.; Walker, A. V. Investigation of the Mechanism of Nickel Electroless Deposition on Functionalized Self-Assembled Monolayers. *Langmuir* **2011**, *27*, 6932−6939.

(18) Lu, P.; Shi, Z.; Walker, A. V. Selective Electroless Deposition of Copper on Organic Thin Films with Improved Morphology. *Langmuir* **2011**, *27*, 13022−13028.

(19) Schlesinger, M.; Paunovic, M. *Modern Electroplating*, 4th ed.; John Wiley & Sons: New York, 2000.

(20) Hammami, O.; Dhouibi, L.; Berçot, P.; Rezrazi, E. M.; Triki, E. Effect of diethanolamine and triethanolamine on the properties of electroplated Zn−Ni alloy coatings from acid bath. *Can. J. Chem. Eng.* **2013**, *91*, 19−26.

(21) Shingubara, S.; Wang, Z.; Yaegashi, O.; Obata, R.; Sakaue, H.; Takahagi, T. Bottom-Up Fill of Copper in Deep Submicrometer Holes by Electroless Plating. *Electrochem. Solid-State Lett.* **2004**, *7*, C78−C80.

DOI: 10.1021/acs.langmuir.7b03725
Langmuir 2018, 34, 4142−4149

(22) Tan, M.; Guymon, C.; Wheeler, D. R.; Harb, J. N. The Role of SPS, MPSA, and Chloride in Additive Systems for Copper Electrodeposition. *J. Electrochem. Soc.* **2007**, *154*, D78−D81.
(23) Lin, K.-C.; Shieh, J.-M.; Chang, S.-C.; Dai, B.-T.; Chen, C.-F.; Feng, M.-S. Electroplating copper in sub-100 nm gaps by additives with low consumption and diffusion ability. *J. Vac. Sci. Technol., B: Microelectron. Nanometer Struct.–Process., Meas., Phenom.* **2002**, *20*, 940−945.
(24) Kondo, K.; Kojima, K.; Ishida, N.; Irie, M. Effects of 2,2′-Dipyridyl on Electroless Copper Deposition in the Presence of Excess Triethanolamine. *J. Electrochem. Soc.* **1993**, *140*, 1598−1601.
(25) Paunovic, M.; Arndt, R. The Effect of Some Additives on Electroless Copper Deposition. *J. Electrochem. Soc.* **1983**, *130*, 794−799.
(26) Moffat, T. P.; Bonevich, J. E.; Huber, W. H.; Stanishevsky, A.; Kelly, D. R.; Stafford, G. R.; Josell, D. Superconformal Electrodeposition of Copper in 500-90 nm Features. *J. Electrochem. Soc.* **2000**, *147*, 4524−4535.
(27) Wang, X.; Li, N.; Yang, Z.; Wang, Z. Effects of Triethanolamine and $K_4[Fe(CN)_6]$ upon Electroless Copper Plating. *J. Electrochem. Soc.* **2010**, *157*, D500−D502.
(28) National Center for Biotechnology Information. PubChem Compound Database; CID=8758. https://pubchem.ncbi.nlm.nih.gov/compound/8758 (accessed Sept 6, 2017 4.00 pm).
(29) National Center for Biotechnology Information. PubChem Compound Database; CID=7618. https://pubchem.ncbi.nlm.nih.gov/compound/7618 (accessed Sept 6, 2017 4.00 pm).
(30) National Center for Biotechnology Information. PubChem Compound Database; CID=24730. https://pubchem.ncbi.nlm.nih.gov/compound/24730 (accessed Sept 6, 2017 4.00 pm).
(31) Kremer, C. B. The ethanolamines. *J. Chem. Educ.* **1942**, *19*, 80.
(32) Dow Ethanolamines. http://msdssearch.dow.com/PublishedLiteratureDOWCOM/dh_0044/0901b8038004475c.pdf?filepath=amines/pdfs/noreg/111-01375.pdf&fromPage=GetDoc (accessed Sept 7, 2017 4.15pm).
(33) Bolling, J. M.; Hall, J. L. Spectrophotometric Investigation of the Copper(II) Ion-Triethanolamine Complex. *J. Am. Chem. Soc.* **1953**, *75*, 3953−3955.
(34) Fisher, J. F.; Hall, J. L. Polarographic study of complexes of copper(II) ion with ammonia and various ethyl, ethanol, and ethylethanol-amines. *Anal. Chem.* **1967**, *39*, 1550−1556.
(35) Davies, C. W.; Patel, B. N. Complexes of the cupric ion with mono-, di-, and tri-ethanolamine. *J. Chem. Soc. A* **1968**, 1824−1828.
(36) Tauler, R.; Casassas, E.; Rode, B. M. The complex formation of Cu(II) with mono- and di-ethanolamine in aqueous solution. *Inorg. Chim. Acta* **1986**, *114*, 203−209.
(37) Tauler, R.; Casassas, E.; Rainer, M. J. A.; Rode, B. M. The complex formation of Cu(II) with triethanolamine in aqueous solution. *Inorg. Chim. Acta* **1985**, *105*, 165−170.
(38) Casassas, E.; Tauler, R. Potentiometric Study of Mixed Ligand Complex Formation in the Copper(II)-Salicylate-Mono, Di-, and Triethanolamine Systems. *J. Chim. Phys. Phys.-Chim. Biol.* **1986**, *83*, 409−417.
(39) Casassas, E.; Gustems, L. L.; Tauler, R. Spectrophotometric study of complex formation in copper(II) mono-, di-, and triethanolamine systems. *J. Chem. Soc., Dalton Trans.* **1989**, 569−573.
(40) Tutunaru, B.; Samide, A. The Study on the Influence of Aminic Additive in the Tin Electro-Deposition Process on the Carbon Steel Surface from the Alkaline bath. *J. Optoelectron. Adv. Mater.* **2008**, *2*, 659−665.
(41) National Center for Biotechnology Information. PubChem Compound Database; CID=700. https://pubchem.ncbi.nlm.nih.gov/compound/700 (accessed Sept 6, 2017 4.00 pm).
(42) National Center for Biotechnology Information. PubChem Compound Database; CID=8113. https://pubchem.ncbi.nlm.nih.gov/compound/8113 (accessed Sept 6, 2017 4.00 pm).
(43) Ulman, A. Formation and structure of self-assembled monolayers. *Chem. Rev.* **1996**, *96*, 1533−1554.
(44) Schreiber, F. Structure and growth of self-assembling monolayers. *Prog. Surf. Sci.* **2000**, *65*, 151−257.
(45) Dubois, L. H.; Nuzzo, R. G. Synthesis, Structure, and Properties of Model Organic Surfaces. *Annu. Rev. Phys. Chem.* **1992**, *43*, 437−463.
(46) Fisher, G. L.; Walker, A. V.; Hooper, A. E.; Tighe, T. B.; Bahnck, K. B.; Skriba, H. T.; Reinard, M. D.; Haynie, B. C.; Opila, R. L.; Winograd, N.; Allara, D. L. Bond Insertion, Complexation and Penetration Pathways of Vapor-Deposited Aluminum Atoms with HO- and CH_3O- Terminated Organic Monolayers. *J. Am. Chem. Soc.* **2002**, *124*, 5528−5541.
(47) Hooper, A.; Fisher, G. L.; Konstadinidis, K.; Jung, D.; Nguyen, H.; Opila, R.; Collins, R. W.; Winograd, N.; Allara, D. L. Chemical Effects of Methyl and Methyl Ester Groups on the Nucleation and Growth of Vapor-Deposited Aluminum Films. *J. Am. Chem. Soc.* **1999**, *121*, 8052−8064.
(48) Nagy, G.; Walker, A. V. Dynamics of the Interaction of Vapor-Deposited Copper with Alkanethiolate Monolayers: Bond Insertion, Complexation and Penetration Pathways. *J. Phys. Chem. B* **2006**, *110*, 12543−12554.
(49) Walker, A. V.; Tighe, T. B.; Cabarcos, O. M.; Reinard, M. D.; Haynie, B. C.; Uppili, S.; Winograd, N.; Allara, D. L. The Dynamics of Noble Metal Atom Penetration Through Methoxy-Terminated Alkanethiolate Monolayers. *J. Am. Chem. Soc.* **2004**, *126*, 3954−3963.
(50) The Royal Society of Chemistry Data Book Website; Datasheets Stability Constants for Metal Ion Complexes. http://www.rsc.org/education/teachers/resources/databook/ds_stability_constants.htm (accessed Sept 6, 2017 4.30pm).
(51) Mallory, G. O.; Hajdu, J. B. *Electroless Plating: Fundamentals and Applications*; Noyes Publications/William Andrew Publishing, LLC: Norwich, NY, 1990.
(52) Ellsworth, A. A.; Walker, A. V. From Nanowires to Nanopores: A Versatile Method for Electroless Deposition of Nanostructures on Micropatterned Organic Substrates. *Langmuir* **2016**, *32*, 2668−2674.
(53) Shi, Z.; Walker, A. V. Synthesis of Nickel Nanowires via Electroless Nanowire Deposition on Micropatterned Substrates. *Langmuir* **2011**, *27*, 11292−11295.
(54) Lelental, M. Dimethylamine Borane as the Reducing Agent in Electroless Plating Systems. *J. Electrochem. Soc.* **1973**, *120*, 1650−1654.
(55) Israéli, Y. J. Formation Constants of Some Mixed Complexes resulting from the Reaction of Disodium Nitrilotriacetate with Metal Versenates (EDTA). *Nature* **1964**, *201*, 389−390.
(56) Smith, G. S.; Hoard, J. L. The Structure of Dihydrogen Ethylenediaminetetraacetatoaquonickel(II). *J. Am. Chem. Soc.* **1959**, *81*, 556−561.

DOI: 10.1021/acs.langmuir.7b03725
Langmuir 2018, 34, 4142−4149